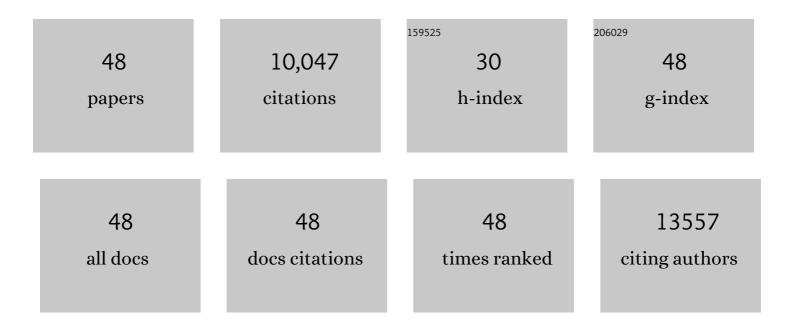
Wei Chen

List of Publications by Year in descending order

Source: https://exaly.com/author-pdf/2985819/publications.pdf Version: 2024-02-01



#	Article	IF	CITATIONS
1	Boosting the catalytic activity of a step-scheme In2O3/ZnIn2S4 hybrid system for the photofixation of nitrogen. Chinese Journal of Catalysis, 2022, 43, 265-275.	6.9	67
2	Synergistic effects of interface coupling and defect sites in WO3/InVO4 architectures for highly efficient nitrogen photofixation. Separation and Purification Technology, 2022, 290, 120875.	3.9	31
3	Flower-like ZnIn2S4 microspheres with highly efficient catalytic activity for visible-light-driven sulfamethoxazole photodegradation. Colloids and Surfaces A: Physicochemical and Engineering Aspects, 2022, 643, 128779.	2.3	18
4	Fabrication of direct Z-scheme FeIn2S4/Bi2WO6 hierarchical heterostructures with enhanced photocatalytic activity for tetracycline hydrochloride photodagradation. Ceramics International, 2021, 47, 6318-6328.	2.3	69
5	Multifunctional graphene-based nano-additives toward high-performance polymer nanocomposites with enhanced mechanical, thermal, flame retardancy and smoke suppressive properties. Chemical Engineering Journal, 2021, 410, 127590.	6.6	101
6	Step-scheme WO3/CdIn2S4 hybrid system with high visible light activity for tetracycline hydrochloride photodegradation. Applied Surface Science, 2021, 535, 147682.	3.1	122
7	Accelerated photocatalytic degradation of tetracycline hydrochloride over CuAl2O4/g-C3N4 p-n heterojunctions under visible light irradiation. Separation and Purification Technology, 2021, 277, 119461.	3.9	110
8	Direct Z-scheme 1D/2D WO2.72/ZnIn2S4 hybrid photocatalysts with highly-efficient visible-light-driven photodegradation towards tetracycline hydrochloride removal. Journal of Hazardous Materials, 2020, 384, 121308.	6.5	171
9	Mechanistic Study of Monolayer NiP ₂ (100) toward Solar Hydrogen Production. Solar Rrl, 2020, 4, 1900360.	3.1	8
10	Highly efficient visible-light-driven photocatalytic hydrogen evolution by all-solid-state Z-scheme CdS/QDs/ZnIn2S4 architectures with MoS2 quantum dots as solid-state electron mediator. Applied Surface Science, 2020, 504, 144406.	3.1	61
11	A new strategy to immobilize molecular Fe sites into a cationic polymer to fabricate an oxygen reduction catalyst. Electrochemistry Communications, 2020, 117, 106781.	2.3	1
12	Direct Z-scheme CdFe2O4/g-C3N4 hybrid photocatalysts for highly efficient ceftiofur sodium photodegradation. Journal of Materials Science and Technology, 2020, 56, 133-142.	5.6	100
13	Nitrogen and sulfur dual-doped carbon nanotube derived from a thiazolothiazole based conjugated microporous polymer as efficient metal-free electrocatalysts for oxygen reduction reaction. Journal of Power Sources, 2020, 461, 228145.	4.0	29
14	Mesoporous Bi2MoO6 quasi-nanospheres anchored on activated carbon cloth for flexible all-solid-state supercapacitors with enhanced energy density. Journal of Power Sources, 2020, 463, 228202.	4.0	24
15	Efficient and stable charge transfer channels for photocatalytic water splitting activity of CdS without sacrificial agents. Journal of Materials Chemistry A, 2020, 8, 20963-20969.	5.2	95
16	Catalytically Active Sites on Ni5P4 for Efficient Hydrogen Evolution Reaction From Atomic Scale Calculation. Frontiers in Chemistry, 2019, 7, 444.	1.8	15
17	Realizing simultaneous improvements in mechanical strength, flame retardancy and smoke suppression of ABS nanocomposites from multifunctional graphene. Composites Part B: Engineering, 2019, 177, 107377.	5.9	117
18	Mesoporous g-C3N4 ultrathin nanosheets coupled with QDs self-decorated SnIn4S8 homojunctions towards highly efficient photocatalytic functional transformation. Journal of Alloys and Compounds, 2019, 809, 151859.	2.8	17

Wei Chen

#	Article	IF	CITATIONS
19	Stable Active Sites on Ni 12 P 5 Surfaces for the Hydrogen Evolution Reaction. Energy Technology, 2019, 7, 1900013.	1.8	7
20	Direct Z-scheme 2D/2D MnIn2S4/g-C3N4 architectures with highly efficient photocatalytic activities towards treatment of pharmaceutical wastewater and hydrogen evolution. Chemical Engineering Journal, 2019, 359, 244-253.	6.6	194
21	Hydrothermal route to synthesize helical CdS@ZnIn2S4 core-shell heterostructures with enhanced photocatalytic hydrogeneration activity. Ceramics International, 2019, 45, 1803-1811.	2.3	34
22	Self-assembled MoS ₂ -GO Framework as an Efficient Cocatalyst of CuInZnS for Visible-Light Driven Hydrogen Evolution. ACS Sustainable Chemistry and Engineering, 2018, 6, 4671-4679.	3.2	44
23	Anisotropic Electronic Characteristics, Adsorption, and Stability of Low-Index BiVO ₄ Surfaces for Photoelectrochemical Applications. ACS Applied Materials & Interfaces, 2018, 10, 5475-5484.	4.0	93
24	Scaleâ€Up of BiVO ₄ Photoanode for Water Splitting in a Photoelectrochemical Cell: Issues and Challenges. Energy Technology, 2018, 6, 100-109.	1.8	49
25	Enhanced Charge Transport and Increased Active Sites on α-Fe ₂ O ₃ (110) Nanorod Surface Containing Oxygen Vacancies for Improved Solar Water Oxidation Performance. ACS Omega, 2018, 3, 14973-14980.	1.6	36
26	The Influence of Ti Doping on Morphology and Photoelectrochemical Properties of Hematite Grown from Aqueous Solution for Water Splitting. Energy Technology, 2018, 6, 2188-2199.	1.8	18
27	Hybrid of AgInZnS and MoS 2 as efficient visible-light driven photocatalyst for hydrogen production. International Journal of Hydrogen Energy, 2017, 42, 12254-12261.	3.8	26
28	ZnIn 2 S 4 hybrid with MoS 2 : A non-noble metal photocatalyst with efficient photocatalytic activity for hydrogen evolution. Powder Technology, 2017, 315, 157-162.	2.1	47
29	Two-dimensional mesoporous g-C 3 N 4 nanosheet-supported MgIn 2 S 4 nanoplates as visible-light-active heterostructures for enhanced photocatalytic activity. Journal of Catalysis, 2017, 349, 8-18.	3.1	113
30	NbS ₂ Nanosheets with M/Se (M = Fe, Co, Ni) Codopants for Li ⁺ and Na ⁺ Storage. ACS Nano, 2017, 11, 10599-10607.	7.3	95
31	Theoretical Insight into the Mechanism of Photoelectrochemical Oxygen Evolution Reaction on BiVO ₄ Anode with Oxygen Vacancy. Journal of Physical Chemistry C, 2017, 121, 18702-18709.	1.5	89
32	Ultrasound-assisted growth of Zn0.2Cd0.8S nanoparticles on mesoporous P-doped graphitic carbon nitride nanosheets for superior photocatalytic activities. Journal of Alloys and Compounds, 2017, 690, 503-511.	2.8	17
33	Au/ZnO nanoarchitectures with Au as both supporter and antenna of visible-light. Applied Surface Science, 2017, 392, 616-623.	3.1	48
34	Biomolecule-assisted solvothermal synthesis and enhanced visible light photocatalytic performance of Bi2S3/BiOCl composites. Journal Wuhan University of Technology, Materials Science Edition, 2016, 31, 765-772.	0.4	14
35	Hierarchical CdIn2S4 microspheres wrapped by mesoporous g-C3N4 ultrathin nanosheets with enhanced visible light driven photocatalytic reduction activity. Journal of Hazardous Materials, 2016, 320, 529-538.	6.5	102
36	Titania-on-gold nanoarchitectures for visible-light-driven hydrogen evolution from water splitting. Journal of Materials Science, 2016, 51, 6987-6997.	1.7	15

Wei Chen

#	Article	IF	CITATIONS
37	Novel mesoporous P-doped graphitic carbon nitride nanosheets coupled with ZnIn ₂ S ₄ nanosheets as efficient visible light driven heterostructures with remarkably enhanced photo-reduction activity. Nanoscale, 2016, 8, 3711-3719.	2.8	223
38	Well-dispersed ultrafine nitrogen-doped TiO 2 with polyvinylpyrrolidone (PVP) acted as N-source and stabilizer for water splitting. Journal of Energy Chemistry, 2016, 25, 1-9.	7.1	28
39	Several recent designs or choices of nanomaterials for photocatalysis: Ag/AgCl composite, silicate and Bi2MoO6. SPR Nanoscience, 2016, , 211-275.	0.3	3
40	In situ fabrication of novel Z-scheme Bi 2 WO 6 quantum dots/g-C 3 N 4 ultrathin nanosheets heterostructures with improved photocatalytic activity. Applied Surface Science, 2015, 355, 379-387.	3.1	141
41	Synthesis of homogeneous one-dimensional Ni x Cd1â°x S nanorods with enhanced visible-light response by ethanediamine-assisted decomposition of complex precursors. Journal of Materials Science, 2015, 50, 3920-3928.	1.7	28
42	Fabrication of Bi2MoO6 nanoplates hybridized with g-C3N4 nanosheets as highly efficient visible light responsive heterojunction photocatalysts for Rhodamine B degradation. Materials Science in Semiconductor Processing, 2015, 35, 45-54.	1.9	53
43	One-pot hydrothermal route to synthesize the ZnIn2S4/g-C3N4 composites with enhanced photocatalytic activity. Journal of Materials Science, 2015, 50, 8142-8152.	1.7	56
44	A novel yet simple strategy to fabricate visible light responsive C,N-TiO ₂ /g-C ₃ N ₄ heterostructures with significantly enhanced photocatalytic hydrogen generation. RSC Advances, 2015, 5, 101214-101220.	1.7	63
45	Fast preparation of fluorescent carbon nanoparticles from β-cyclodextrin via precursor design treatment. Materials Letters, 2015, 139, 122-125.	1.3	6
46	Fabrication of highly visible light sensitive graphite-like C3N4 hybridized with Zn0.28Cd0.72S heterjunctions photocatalyst for degradation of organic pollutants. Journal of Environmental Chemical Engineering, 2014, 2, 1889-1897.	3.3	22
47	Commentary: The Materials Project: A materials genome approach to accelerating materials innovation. APL Materials, 2013, 1, .	2.2	6,913
48	Evidence for the Active Species Involved in the Photodegradation Process of Methyl Orange on TiO ₂ . Journal of Physical Chemistry C, 2012, 116, 3552-3560.	1.5	314